PROCEEDINGS OF SCIENCE

High energy neutrino astronomy

Emilio Migneco
Dipartimento di Fisica e Astronomia,
Universitá di Catania and
Laboratori Nazionali del Sud - INFN
Via S. Sofia 62 I-95123 Catania, Italy
E-mail: migneco@lns.infn.it

Neutrinos are very promising probes for high energy astrophysics. Indeed, many indications suggest that cosmic objects where acceleration of charged particles takes place, e.g. GRBs and AGNs, are the sources of the detected UHECRs. Accelerated hadrons, interacting with ambient gas or radiation, can produce HE neutrinos. Contrarywise to charged particles and TeV gamma rays, neutrinos can reach the Earth from far cosmic accelerators, traveling in straight line, therefore carrying direct information on the source. Theoretical models indicate that a detection area of $\approx$1 km^2 is required for the measurement of HE cosmic ν fluxes. The detection of Cherenkov light emitted by the secondary leptons produced by neutrino intercation in large volume transparent natural media (water or ice) is today considered the most promising experimental approach to build high energy neutrino detectors. The experimental efforts towards the opening of the high energy neutrino astronomy are also reviewed.

Ettore Majorana's legacy and the Physics of the XXI century
October 5-6, 2006
Catania, Italy

PoS(EMC2006)012

1. Introduction

The first investigations on cosmic rays (CR) date back to the beginning of 20th century. However, many problems concerning their origin are still unsolved. The most recent measurements show that the CR flux extends over 10 orders of magnitude in energy, up to 3×10^{20} eV, and over 28 orders of magnitude in flux, down to few particles per 100 km^2 per century.

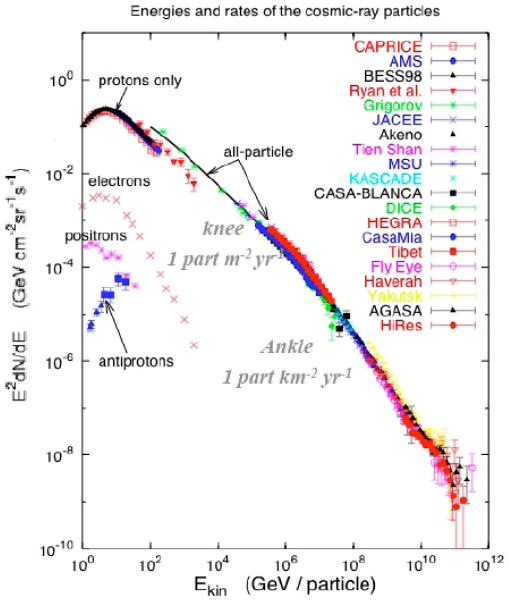

Figure 1: All particle cosmic ray spectrum.

The lower energy region of CR spectrum (E_{CR} <GeV) is well explained by solar activity, while at higher energy there is not direct evidence of connection with sources. Cosmic Ray flux is mostly composed by charged particles and Galactic magnetic field ($B \sim 3\ \mu$G) randomises their arrival direction at the Earth. This implies that the reconstruction of charged CR direction is not possible for particle with energy lower than $E \simeq 10^{20}$ eV. On the other hand neutrons have a decay length (roughly 10 kpc at $E_\nu \simeq 10^{18}$ eV) which is too short to reach the Earth from far sources.

The bulk of CR spectrum is consistent with the Fermi acceleration mechanism [1], whose theoretical description was revised in a more effective version by Bell [2]. It takes place in sources where plasma (e^+e^- or/and pe) contained by strong magnetic fields, is driven by strong shock waves. The spectrum of Fermi accelerated particles follows an $E^{-(2\div 2.2)}$ power law and the maximum energy that a particle can reach is a function of confinement time within the shock:

$$E_{max} \approx \beta_{shock}\, Z\, B\, R, \tag{1.1}$$

where Z is the nucleus atomic number, $\beta_{shock} \times c$ is the shock wave velocity, B and R are the source magnetic field and the source linear extension respectively. Plugging in eq.(1.1) the values of our galaxy, one realizes that Galactic sources cannot accelerate protons to extremely high energies.

The experimental CR spectrum shows a peculiar behavior: at $E > 10^{14.5}$ eV the CR flux changes its spectral index α from $\alpha \simeq 2.7$ to $\alpha \simeq 3.0$ and its composition, from proton-dominated

to nuclei-dominated: the higher the energy, the heavier are the nuclei. This region is called the *knee*. At $E > 10^{18.5}$ eV (the *ankle* region) the CR spectrum features change again. Above this energy the CR flux similar to the pre-knee region: the spectral index $\simeq$2.7 and the flux is proton-dominated. The standard paradigm is that CR flux below the ankle is originated by galactic sources and the change in chemical composition is attributed to the escape of HE protons from the the Milky Way [1]. Since Galactic sources cannot accelerate particles to extremely high energies (as shown in equation 1.1), the detection of cosmic protons with energies up to $E > 10^{19}$ eV suggests the presence of extragalactic sources in which the Fermi acceleration mechanism takes place.

Indeed, the major questions of the astroparticle physics concern the identification of the sources of the most energetic cosmic rays and of their acceleration mechanism, and the puzzle of the detection of CR at energy beyond the GZK cut off.

According to equation 1.1 there are only few classes of cosmic objects capable to accelerate protons at $E >$EeV, among these Gamma Ray Bursters (GRB) [3] and powerful Active Galactic Nuclei (AGN) [4] are the most favourite candidates. These sources, the most luminous bursting ($L_{GRB} \simeq 10^{53}$ erg/sec) and steady ($L_{AGN} \simeq 10^{46}$ erg/s) objects in the Universe, are typically located at cosmological distance. Protons having $E > 10^{20}$ eV possibly accelerated in AGNs and GRBs, could be good astrophysical probes being only slightly bent by cosmic magnetic fields but, at these energies, they are absorbed in the Universe through the interaction with Cosmic Microwave Background Radiation (CMBR), the so called GZK effect [5]. The cross section of the process $p + \gamma \rightarrow \Delta^+$ is $\sigma_{p\gamma} \sim 100$ μbarn and the average CMBR density is $n_{CMBR} \sim 400$ cm^{-3}, therefore the absorption length of UHE protons in the Universe is roughly:

$$L_{p,CMBR} \simeq (\sigma_{p\gamma} \cdot n_{CMBR})^{-1} < 50 \text{ Mpc}. \tag{1.2}$$

High energy (TeV) gamma rays are also produced in the discussed sources. In fact, protons accelerated via Fermi mechanism can interact, within the source or in its vicinity, with gas clouds or inter-stellar medium (pp) and with ambient radiation ($p\gamma$) producing pions; neutral pions then decay into high energy gammas. HE gamma rays can also be generated by purely electromagnetic mechanisms via electron Bremstrahalung and Inverse Compton Scattering, as supposed in the case of close ($\leq$ 100 Mpc) AGNs Mkn-421 and Mkn-501 [6]. Very impressive data on gamma TeV sources has been collected with the air Cherenkov telescope array HESS and a lot of the observations concern the region of the Galactic centre. Several sources are not identified since they have not a counterpart in other wavelengths [7]. More recently also the MAGIC telescope provided interesting data on gamma TeV sources, confirming the HESS results for the sources which can be observed from both the instruments. Gamma spectra show an E^{-2} dependence consistent with hadronic interactions [8]. The neutrino flux, produced by charged pion decay, is expected to be similar to the hadronic high energy gamma one. The possibility of neutrino detection from these TeV gamma sources represents a unique tool to provide a conclusive answer on the role of hadronic and electromagnetic processes. However, the detection of $E_\gamma \simeq 10$ TeV rays from point-like sources is limited to few tens Mpc, due to pair production interaction of HE gamma rays with diffuse infrared and microwave cosmic background.

[1] The gyroradius of $E > 10^{17}$ eV protons is larger than Galaxy thickness ($\simeq$ 50 pc), moreover due to the effect of galactic magnetic field fluctuations, protons leave our Galaxy even at smaller energies. At the same energies heavier nuclei, with larger Z, are confined.

In this scenario only high energy neutrinos offer the possibility to directly observe TeV÷PeV radiation emitted by far cosmic objects. Thus, the observation of cosmic HE neutrinos can probe hadronic processes and hopefully extend our understanding of the more violent phenomena occuring in the far Universe.

2. High energy neutrino production

Hadronic source models predict that, in cosmic objects, high energy pions are produced (directly or through Δ resonance) by pp or $p\gamma$ interactions (photomeson production). While neutral pions decay into gamma rays, neutrinos are generated through decay chains of charged pions. If the muon cooling time in the source is larger than their decay time, high energy electron neutrinos are also produced through the reaction chains:

$$\begin{array}{rl} & \pi_0 \rightarrow \gamma+\gamma \\ & \Big\uparrow \\ p+p,\gamma \rightarrow N+ & \pi \\ & \Big\downarrow \\ & \pi^{\pm} \rightarrow \nu_\mu+\mu \\ & \qquad\qquad \Big\downarrow \\ & \qquad\quad \mu \rightarrow e+\nu_\mu+\nu_e. \end{array} \tag{2.1}$$

In a first guess, the source ν spectrum is expected to follow the primary protons one (E^{-2}), with a fraction of proton energy going into pions of roughly 0.2 and $E_\nu \simeq 0.05\ E_p$. The reaction chains 2.1 also predict that ν_μ and ν_e are produced in a ratio of 2:1. Taking into account $\nu_\mu \leftrightarrow \nu_\tau$ oscillations and assuming present experimental values of Δm^2 and $\sin^2\theta$ [9] equipartition between the three leptonic flavours is expected at the Earth.

A number of astrophysical high energy neutrino sources have been suggested as neutrino candidates. Indeed, $p\gamma$ interactions are expected to occur in several astrophysical environments.

In Supernova remnants (SNRs) protons, accelerated through Fermi mechanism, can interact with gas in dense SN shells, producing both neutral and charged pions [10]. $p\gamma$ interactions can occur in astrophysical environments that show dense low energy photons fields: microquasar (μQSO) jets [11], AGNs (blazars and BL Lacs [12, 13]) and in GRBs [14] are examples. AGNs and GRBs are particularly relevant since they are the candidate sources of UHECR. Starting from this hypothesis Waxman and Bahcall set an upper bound (the so called WB limit) to high energy neutrino fluxes that can reach the Earth [15, 16]. The limit is obtained assuming that the energy density injection rate of $10^{19} \div 10^{21}$ eV CRs is $\simeq 10^{44.5}$ erg Mpc^{-3}year^{-1}, assuming that particles are accelerated at their sources with E^{-2} spectrum, and posing, conservatively, that pions carry a fraction of proton energy $f_\pi < 1$ and neutrinos carry about 1/4 of this amount. The resulting upper limit for diffuse neutrino flux is:

$$E_\nu^2 \Phi_\nu \simeq \frac{c}{4\pi}\frac{f_\pi}{4} E_p^2 \left(\frac{dN_p}{dE_p dt}\right) t_{Hubble} \simeq 10^{-7.5} \text{GeV /(cm}^2 \text{ s sr)} \tag{2.2}$$

This limit has been discussed and recalculated by Mannheim, Protheroe, Rachen [17] and, again, by Waxman and Mannheim [18], taking into account the effect of propagation of CR and of cos-

mological evolution of the source distribution. However equation 2.2 limit sets a strong reference value for the discussions on the dimensions of future neutrino telescopes.

Astrophysical objects that do not contribute to UHECR spectrum are not constrained by the WB limit. In *optically thick* sources (for which the optical depth is $\tau_{p\gamma} \equiv R_{source} \cdot (\sigma_{p\gamma} n_\gamma) \gg 1$) all nucleons interact while neutrinos can escape giving rise to a ν flux not constrained by relation 2.2. The advantage of Galactic sources observation is due to the fact that though they are much fainter than extragalactic sources ($L_{\mu QSO} \simeq 10^{33}$ erg/s) they are close to the Earth and can therefore produce observable neutrino fluxes. In μQSO, for instance, photomeson interaction of PeV protons on ambient X synchrotron radiation could produce directional neutrino fluxes at Earth [19]. Waxman-Bahcall limit does not apply also to a different kind of processes, known as *top-down*, which foresee the production of high energy CR, gammas and neutrinos by the decay or annihilation of particles with mass $M_X > 10^{21}$ eV, relics of the primordial Universe such as Topological Defects or GUT scale WIMPS (for an exhaustive review see [20]).

3. High energy neutrino astronomy

As shown in the previous section, light and neutral neutrinos are optimal probes for high energy astronomy, i.e. for the identification of astrophysical sources of UHE particles. To fulfill this task neutrino detectors must be design to optimise reconstruction of particle direction and energy, thus they are commonly referred as *neutrino telescopes* (for a clear review see [10]).

HE neutrinos are detected indirectly following weak Charged Current (CC) interaction with nucleons in matter and the production of a charged lepton in the exit channel of the reaction. The low νN cross section ($\sigma_{\nu N} \simeq 10^{-35}$ cm^2 at $\simeq$1 TeV) and the expected astrophysical ν fluxes intensities require a ν interaction target greater than 1 GTon. Markov and Zheleznykh proposed the use of natural water (lake or seawater or polar ice) to detect neutrinos [21] using the optical Čerenkov technique to track the charged lepton outgoing the νN interaction. Underwater neutrino telescopes are, then, large arrays of optical sensors (typically photomultipliers tubes of about 10" diameter) which permit charged leptons tracking in water by timing the Čerenkov wavefront emitted by the particle.

When an upward going particle is reconstructed this is a signature of neutrino event, since the atmospheric upgoing muon background is completely filtered by the Earth. Seawater has a threefold use: huge (and inexpensive) neutrino target, Čerenkov light radiator and shielding for cosmic muon background.

Neutrino weak interaction cross section is dominated at $E_\nu > 100$ GeV by charged current Deep Inelastic Scattering (DIS) [22]

$$\nu_l + N \rightarrow l + X \tag{3.1}$$

where l is the lepton flavor ($l = e, \mu, \tau$), N represents the hit nucleon, X the outgoing hadron(s). The $\nu + N$ CC cross section increases linearly with neutrino energy up to $\simeq 5$ TeV energy, above this value its slope changes to $E^{0.4}$. This leads to two implications: a) the number of detectable neutrino-induced events increase with energy; b) the absorption length of neutrinos in the Earth

$$L_{\nu N} \simeq (\sigma_{\nu N}^{total} < \rho Earth >)^{-1} \tag{3.2}$$

is, for $E \geq$100 TeV, comparable to the Earth diameter.

Underwater and underice neutrino telescopes are expected to identify lepton flavor by reconstructing event topology due to different propagation of e, μ and τ in water. Among different flavors, muon detection is favored. Muons take, in average $50 \div 60\%$ of neutrino energy and μ-range in water is, at $E \simeq$ TeV, of the order of kilometres. Muon neutrino detection allows neutrino astronomy: the angle between the outgoing muon and the interacting neutrino decreases as a function of neutrino energy. At high energy the muon track is therefore almost co-linear to the neutrino one and allows pointing back to the ν cosmic source.

In order to calculate the number of detectable events expected by cosmic neutrinos it is important to introduce the quantity $P_{\nu\mu}$, which is the probability to convert a neutrino into a detectable muon. This probability is a function of the neutrino interaction cross section and of the average muon range $R(E_\mu, E_\mu^{min})$:

$$P_{\mu\nu}(E_\nu) = N_A \int_{E_\mu^{min}}^{E_\nu} dE\mu \frac{d\sigma_{\nu N}^{CC}}{dE\mu} R(E_\mu), \tag{3.3}$$

where N_A is the Avogadro number and E_μ^{min} is the minimum detectable muon energy, or detector threshold. For a given detector the value of $P_{\mu\nu}$ has to be calculated via numerical simulations [10]. As a rule of thumb $P_{\mu\nu} \simeq 1.3 \times 10^{-6}$ for TeV neutrinos ($E_\mu^{min} = 1$ GeV) and increases with energy [2] as $E^{0.8}$. Since, in the energy range of interest, the muon range is of the order of kilometres, and even larger, detectable muons can be originated far from the detector volume. The parameter usually quoted to describe detector performances is the detector *effective area* A_{eff} for muons, i.e. the surface intersecting the neutrino-induced muon flux folded with the detection efficiency for muons. The rate of events produced by a neutrino flux $\Phi_\nu(E_\nu, \vartheta)$ per unit of detector effective area, is then expressed by

$$\frac{N_\mu(E_\mu^{min}, \vartheta)}{A_{eff}\, T} = \int_{E_\mu^{min}}^{E_\nu} dE_\nu \Phi_\nu(E_\nu, \vartheta) P_{\nu\mu} e^{-\frac{Z(\vartheta)}{L_{\nu N}(E_\nu)}}, \tag{3.4}$$

$L_{\nu N}$ being the neutrino absorption length in the Earth and $Z(\vartheta)$ the Earth column depth.

Plugging the WB limit flux (see Eq. 2.2) into equation 3.4 and integrating over the solid angle, one gets a rate of about 10^2 upgoing events per year for a 1 km^2 effective area detector with $E_\mu \simeq$1 TeV threshold. This number sets the scale for the size of an astrophysical neutrino detector.

Besides these isotropically distributed events, a number of point-like sources can produce cluster of ν events. Bright AGN blazars could produce intense ν fluxes. Atoyan and Dermer estimated a high energy neutrino flux as high as $E_\nu^{-2}\Phi_\nu \simeq 10^{-10}$ erg cm^{-2}s^{-1} for 3C273 [13]), which can produce $\simeq 10$ detectable muons per year in a km^3 telescope. Close and/or intense GRBs, like the well known GRB-030329, are also expected to be detected as point sources (some muon events per burst [23] in a km^2). In the GRB case time and direction coincidence between νs and MeV γs will permit effective atmospheric ν background rejection, enhancing the detector discovery capabilities. Bednarek calculated a neutrino flux from the Crab SNR of $E_\nu^{-2}\Phi_\nu \simeq 10^{-10}$ erg cm^{-2}s^{-1}, this flux could produce few muon events per year in a km^2 detector [24]. A larger number of events, up to some tens or hundreds, is expected from several Galactic microquasars:

[2] For $E_\nu \gg E_\mu^{min}$ the $P_{\mu\nu}$ shape is independent on E_μ^{min}

SS433 and GX339-4, in particular, are expected to emit ν fluxes of the order 10^{-9} erg cm^{-2}s^{-1} [19].

The underwater Čerenkov technique allows the tracking of charged relativistic particles. In water (whose refractive index for blue light is $n \simeq 1.35$) Čerenkov photons are emitted along particle track at $\vartheta_{\check{C}} \simeq 42^o$. The time sequence of photons hits on PMTs is correlated by the causality relation

$$c(t_j - t_0) = l_j + d_j \tan(\vartheta_{\check{C}}). \tag{3.5}$$

The space-time pattern of Čerenkov wavefront can be reconstructed in a off-line analysis by fitting relation 3.5 to the data. The reconstructed muon direction will be affected by indetermination on PMTs position (due to underwater position monitoring) and on hit time (PMT transit time spread, detector timing calibration, ...).

Particle energy loss via Čerenkov radiation is only a negligible fraction of the total energy loss and the number of Čerenkov photons emitted by a charged relativistic particle in water is roughly 300 per cm of track. Simulations show that an underwater detector having an instrumented volume of about 1 km^3 equipped with $\simeq$ 5000 optical modules can achieve an affective area of $\simeq$ 1 km^2 and an angular resolution of $\simeq 0.1^\circ$ for $E_\mu > 10$ TeV muons [25]. Indetermination on muon energy is large since the energy loss in Čerenkov light is very small and since only a fraction of the muon track is sampled.

Medium (water or ice) optical properties determine the detector granularity (i.e. the PMT density). Water is transparent only in a narrow range of wavelengths ($350 \leq \lambda \leq 550$ nm). For blue light, such as Čerenkov radiation, the absorption length of clear ocean waters is $L_a \simeq 70$ m. This number roughly sets the spacing distance between PMTs, thus $\simeq$ 5000 PMTs could fill up a volume of one km^3.

The estimate of the detector performances requires detailed MonteCarlo simulations that have to take into account the detector layout and the physical characteristics of the medium constituting and surrounding the detector. Light refraction index, light absorption and scattering coefficients must be accurately measured *in situ* [26].

Neutrino detectors have to identify faint astrophysical neutrino fluxes among a diffuse atmospheric background. The cosmic muon flux, which at sea surface is about 10 orders of magnitude higher than the number of neutrino-induced upgoing muons, strongly decreases below sea surface as a function of depth and of the zenith angle: it falls to zero near the horizon and below. This is the reason why astrophysical neutrino signals are searched among upward-going muons. At 3000 m depth, an underwater neutrino telescope is hit by a cosmic muon flux still about 10^6 times higher than the upgoing atmospheric neutrino signal, therefore accurate reconstruction procedures are needed to avoid the mis-reconstruction of downgoing tracks as *fake* upgoing.

In the case of the background produced by atmospheric neutrinos, energy cuts and statistical arguments can be used to discriminate these events from astrophysical ones during data analysis. In fact, atmospheric ν flux is expected to produce diffuse events with a known spectral index ($\alpha \simeq -3.7$ at $E_\nu > 10$ TeV) while neutrino fluxes coming from astrophysical point sources are expected to follow an E^{-2} and to be concentrated within a narrow angular region, in the direction of their source, whose dimension is essentially given by the detector angular resolution.

Another background source is the optical noise in seawater. This background is due to the presence of bioluminescent organisms and radioactive isotopes. Radioactive elements in water (mainly ^{40}K) originate electrons above the Čerenkov threshold. ^{40}K decay produces an uncorrelated background on PMTs that has been measured to be about 20÷30 kHz for 10" PMT (at 0.5 single photoelectron -s.p.e.- threshold) [27]. These signals must be eliminated by the event trigger and reconstruction algorithms. Optical noise is also due to bioluminescent organisms living in deep water. These organisms (from small bacteria to fishes) produce long lasting ($\simeq 10^{-3}$ s) bursts of light that saturate close PMTs for the period of emission. In oceanic deep seawater (as measured for example at a depth of 3000 m in the Ionian Sea Plateau) bioluminescent signals are rare (few per hour) and do not affect the average optical noise rate on PMTs. On the contrary, in biologically active waters, bioluminescence signals may produce an intense background noise up to MHz (on 10" PMTs, 0.5 s.p.e) [27]. This high rates strongly worsen the telescope track reconstruction capabilities and, in the worst case, could not be afforded by data-rate transmission.

4. Underwater/ice neutrino telescopes

As shown in previous sections, the expected number of detectable high energy astrophysical neutrino events is from few to 100 per km^2 per year [10] and only detectors with an effective area (A_{eff}) of 1 km^2 scale could allow the identification of their sources. Starting from the second half of '90s, two small scale neutrino telescopes AMANDA [28] ($A_{eff} \simeq 0.1$ km^2) and BAIKAL [29] ($A_{eff} \simeq 10^4$ m^2) demonstrated the possibility to use underwater/ice Čerenkov technique to track $E_\nu > 100$ GeV neutrinos, measuring the atmospheric neutrino spectrum at high energies. The detector design should be optimised in order to get an effective area of $\simeq 1$ km^2 and a pointing accuracy $\lesssim 0.1^\circ$ for 10 TeV muons, an energy resolution of the order of some tens percent in $\log(E)$ and an energy threshold close to 100 GeV.

4.1 The running neutrino telescopes: Baikal-NT and AMANDA

After the pioneering work carried out by the DUMAND collaboration offshore Hawaii Island [30], Baikal was the first collaboration which installed an underwater neutrino telescope and, after more than ten years of operation, it is still the only neutrino telescope located in the Northern Hemisphere. The BAIKAL NT-200 is an array of 200 PMTs, moored between 1000 and 1100 m depth in lake Baikal (Russia) [29]. The deployment and recovery operations are carried out during winter, when a thick ice cap (about 1 meter) is formed over the lake. BAIKAL is an high granularity detector with a threshold $E_\mu \simeq 10$ GeV and an estimated effective detection area $\leq 10^5$ m^2 for TeV muons. The limited depth and the poor qualities of lake water (light transmission length of 15÷20 m, high sedimentation and bio-fouling rate, optical background due to bioluminescence) limit the detector performances as a neutrino telescope. The apparatus is taking data since 1998. The upper limit obtained for a diffuse flux (ν_e+ν_μ+ν_τ) for a E^2 spectrum is $E_\nu^2 \Phi_\nu < 8.1 \times 10^{-7}$ cm^{-2} sec^{-1} sr^{-1} GeV at 90% confidence level [31].

AMANDA [28] is currently the largest neutrino telescope installed. In the present stage, named AMANDA II, the detector consists of 677 optical modules (OM) pressure resistant glass vessel hosting downward oriented PMTs and readout electronics. OMs are arranged in 19 vertical strings, deployed in holes drilled in ice between 1.3 and 2.4 km depth. Vertical spacing between

OMs is 10÷20 m, horizontal spacing between strings is 30÷50 m. The ice optical properties have been mapped as a function of depth: at detector installation depth the average light ($\lambda = 400$ nm) absorption length is $L_a \simeq 100$ m (in the ocean $L_a \simeq 70$ m), the effective light scattering length is $L_b \simeq 20$ m ($L_b > 100$ m in the ocean). This makes AMANDA a good calorimeter for astrophysical events, with a resolution 0.4 in log(E) for muons and 0.15 in log(E) for electron cascades. The detector angular resolution is between 1.5° and 3.5° for muons and $\simeq 30°$ for cascades. AMANDA data have permitted to measure for the first time the upgoing atmospheric neutrino spectrum in the energy range from few TeV to 300 TeV. AMANDA provided the most stringent upper limits on neutrino fluxes. For diffuse astrophysical muon neutrino fluxes ($100 < E_\nu < 300$ TeV) a 90% upper limit $E_\nu^2 \Phi_{\nu_\mu} < 7.8 \times 10^{-7}$ GeV cm^{-2} s^{-1} sr^{-1} was set. For point sources the detector reached a sensitivity $E_\nu^2 \Phi_{\nu_\mu} \simeq 6 \times 10^{-8}$ GeV cm^{-2} s^{-1} calculated, over 807 days live time (years 2000-2003). No indication of either a point-like or a diffuse extraterrestrial flux of TeV neutrinos and beyond has been observed so far.

4.2 IceCube: the underice km^3 neutrino telescope

The IceCube telescope is the natural extension of AMANDA to the km^3 size. When completed (expected in 2010) it will consist of 4800 PMT displaced in 80 strings. All the PMTs will be downward looking and simulations show that an average spacing of 125 m between PMTs is a good compromise between the two requirements of angular resolution $\leq 1°$ ($E_\nu > 1$ TeV) and effective area $\simeq 1$ km^2. Simulations run by the IceCube collaboration show that in three years of live time the detector will reach a sensitivity $E^2 \Phi_\nu = 4 \times 10^{-9}$ GeV cm^{-2} s^{-1} sr^{-1} for a diffuse E^{-2} neutrino spectrum [32]. It is also worthwhile to mention that the under-ice detectors are not affected by radioactive and biological optical noise. This makes them suitable for the search of low energy neutrino fluxes from Galactic SuperNova explosions. Up to now 9 strings were deployed.

4.3 The Mediterranean km^3

The observation of the full sky with at least two neutrino telescopes in opposite Earth Hemispheres is an important issue for the study of transient phenomena. Moreover ν events detection from the Northern Hemisphere is required to observe the Galactic Centre region (not seen by IceCube), already observed by HESS as intense TeV gamma sources. In the Norther Hemisphere a favorable region is offered by the Mediterranean Sea, where several abyssal sites (> 3000 m) close to the coast are present and where it is possible to install the detector near scientific and industrial infrastructures.

An underwater detector offers, compared to IceCube, the possibility to be recovered, maintained and/or reconfigured; detector installation at depth $\geq$3500 m will reduce atmospheric muon background by a factor $\geq$5 with respect to 2000 m depth. The long light scattering length (L_b) of the Mediterranean abyssal seawater preserve the Čerenkov photons directionality and will permit excellent pointing accuracy (order of 0.1° for 10 TeV muons). On the other hand the light absorption length in water (L_a) is shorter than in ice, then it reduces the photon collection efficiency for a single PMT. Differently from deep polar ice, the sea is a biologically active environment where organisms produce background light (bioluminescence). The selection of a marine site with optimal oceanographic and optical parameters is, therefore, a major task for the Mediterranean collaborations involved in the km^3 project.

4.4 Demonstrator detectors: NESTOR and ANTARES

NESTOR [33], the first collaboration that operated in the Mediterranean Sea , proposes to deploy a modular detector at 3800 m depth in the Ionian Sea, near the Peloponnese coast (Greece). Each module is a semi-rigid structure (*the NESTOR tower*), 360 m high and 32 m in diameter, equipped with $\simeq$ 170 PMTs looking both in upward and downward directions. After a long R&D period, during March 2003 NESTOR has successfully deployed 12 PMTs at 3800 m depth acquiring, on-shore, underwater optical noise and cosmic muon signals (745 events reconstructed) for about 1 month. In the next future the collaboration aims at the deployment of the first tower with $\times 10^4$ m^2 effective area for $E_\mu >$10 TeV muons.

ANTARES is a *demonstrator* neutrino telescope with an effective area of 0.1 km^2 for astrophysical ν [34]. It is a high granularity detector consisting of 12 strings, each one made of 25 equidistant stories equipped with 3 PMTs (total 75), placed at an average distance of 60 m. The PMT are 45° downward oriented, in order to avoid their obscuration by sediments and bio-fouling. The detector is located in a marine site near Toulon (France), at 2400 m depth. The collaboration has already deployed a junction box and three lines, two of which are presently connected and operational. The whole detector installation is scheduled to be completed in 2007 [35]. Data recorded by optical modules with the first lines show an unexpectedly high optical background ranging from 60 to several hundreds kHz, well above the one produced by ^{40}K decay, then probably due to bioluminescence.

5. NEMO: Research and Development for the km^3

The construction of km^3 scale neutrino telescopes requires detailed preliminary studies: the choice of the underwater installation site must be carefully investigated to optimize detector performance; the readout electronics must have a very low power consumption; the data transmission system must allow data flow transmission, as high as $\simeq$100 Gbps, to shore; the mechanical design must allow easy detector deployment and recovery operations, moreover the deployed structures must be reliable over more than 10 years which is the estimated life-time of the detector. In order to propose feasible and reliable solutions for the km^3 installation the NEMO (NEutrino Mediterranean Observatory) Collaboration is carrying out an intense R&D activity since 1998 [36].

NEMO intensively studied the oceanographic and optical properties in several deep sea (depth $\geq$ 3000 m) sites close the Italian coast. The results of these campaigns indicate that a large region located 80 km SE of Capo Passero (Sicily) (Fig. 2) is excellent for the installation of the km^3 detector. The bathymetric profile of the region is extremely flat over hundreds km^2, with an average depth of $\simeq$ 3500 m. Deep sea currents are, in the average, as low as 3 cm s^{-1}, and never stronger than 15 cm s^{-1}.

Seawater oceanographic parameters (temperature and salinity) and inherent optical properties (light absorption and attenuation) were measured as a function of depth using a set-up based on the AC9, a commercial transmissometer. The seasonal dependence of the absorption and attenuation lenghts for blue ($\lambda = 440$ nm) light is shown in fig. 3. Values have been averaged over depths of more than 2500 m, where the telescope has to be installed. No significant seasonal effects have

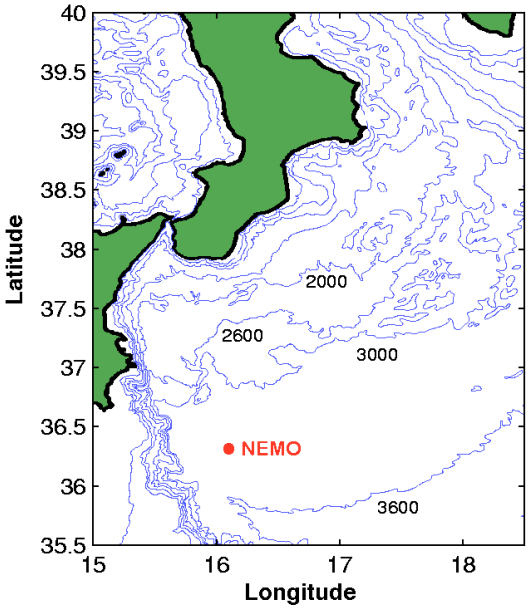

Figure 2: Bathymetry of the Southern Ionian Sea showing the location of the Capo Passero site selected by the NEMO collaboration for the installation of the km^3 detector.

been evidenced. The average value of light absorption length is $L_a = 66 \pm 5$ m [3] close to the value of pure sea water. The same device measured L_a (440nm) $\simeq$ 48 m in the Toulon site [27] and L_a (488nm) $= 27.9 \pm 0.9$ m in the Baikal lake [37].

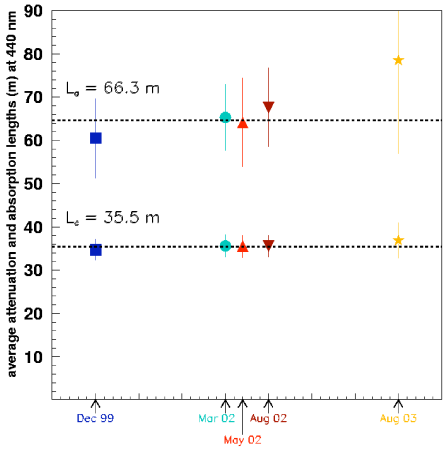

Figure 3: Values of the absorption and attenuation lenghts at 440 nm measured during five different campaigns. The reported values are the average in the depth interval 2850-3250 m.

The optical background noise was also measured at 3000 m depth in Capo Passero. Data collected in Spring 2002 and 2003, for several months, show that optical background induces on

[3] The NEMO Collaboration measured also the value of blue light attenuation length $(L_c^{-1} = L_a^{-1} + L_b^{-1})$ $L_c = 35 \pm 5$ m. Several authors usually quote the water effective scattering length, which is defined as $L_b^{eff} = L_b / < \cos\vartheta >$, where $< \cos\vartheta >$ is the average cosine of the light scattering distribution; in Capo Passero $L_b^{eff} \gg 100$ m.

10" PMTs (0.5 s.p.e.) a constant rate of $20 \div 30$ kHz (compatible with the one expected from ^{40}K decay), with negligible contribution of bioluminescence bursts. These results were confirmed by biological analysis that show, at depth > 2500 m, extremely small concentration of dissolved bioluminescent organisms [27].

5.1 Detector layout and performance

The design of an underwater km^3 neutrino telescope represents a challenging task that has to match many requirements concerning the detector performances, the technical feasibility and the project budget. In general, a km^3 detector is an array of structures each one hosting several tens of optical modules (OM) arranged with a non-homogenous distribution. Moreover, it is important to limit the total number of structures in order to reduce the number of underwater connections. The detector performances were evaluated by means of numerical simulations, carried out using the software [38] developed by the ANTARES collaboration and adapted to km^3 scale detectors [39].

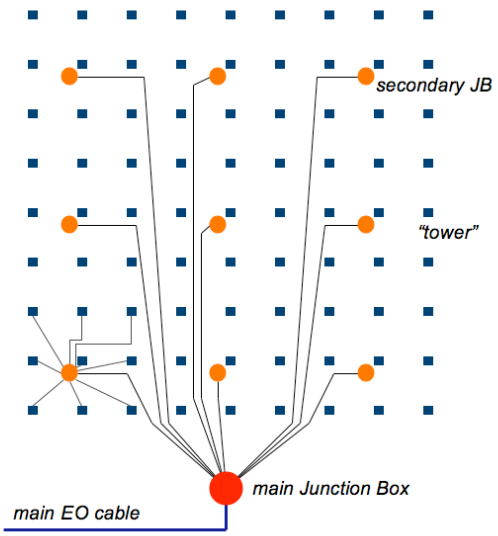

Figure 4: Layout of the proposed NEMO km^3 detector.

The proposed NEMO architecture is a 9×9 square lattice of towers (fig. 4). Details on the structure of the tower will be given in section 6. Here we will just mention that in the simulations a configuration with 18 floors, each one hosting four OMs with 10" PMT was used for a total of 5832 PMTs. The proposed architecture is "modular" and the layout can be reconfigured to match different detector specifications. Site dependent parameters such as depth, optical background, absorption and scattering length, have been set accordingly with the values measured in Capo Passero at a depth of about 3400 m.

The sensitivity of the detector for a generic point-like source is reported in fig. 5 as a function of the integrated data taking time. The source position was chosen at a declination $\delta = -60^\circ$ and a E^{-2} neutrino energy spectrum was considered. For a comparison the IceCube sensitivity [32] obtained for a 1° search bin is also reported in the figure.

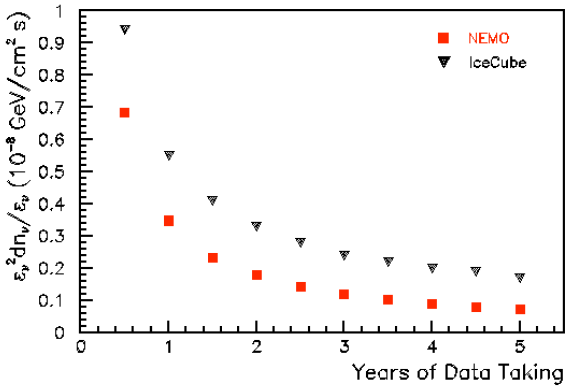

Figure 5: Sensitivity of the NEMO km^3 detector to a neutrino point-like source with declination $\delta = -60°$ and a E^{-2} neutrino energy spectrum compared to the IceCube sensitivity [32].

A study of the Moon shadow effect, due to the absorption of primary cosmic rays by the Moon, has also been undertaken with simulations. Indeed, this effect should provide a direct measurement of both the detector angular resolution and pointing accuracy. Preliminary results [40] show an angular resolution $\sigma = 0.19° \pm 0.02°$.

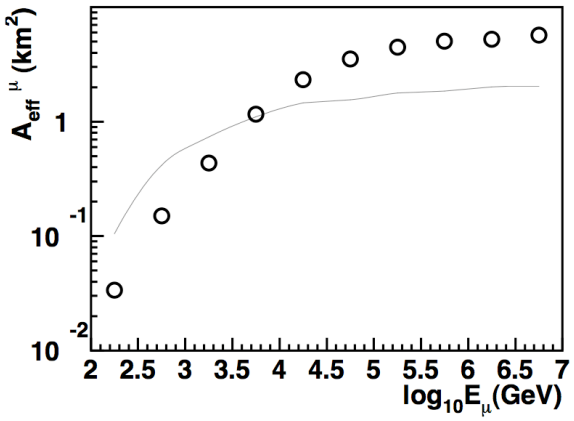

Figure 6: Effective areas for two different configurations of the NEMO km^3 detector: 140 m tower interspacing (solid line) and 300 m tower interspacing (open symbols).

The energy range of interest for high energy neutrino telescopes is very broad, spanning from few hundreds of GeV to very high energies such as the GZK energies ($\sim 10^{20} eV$). Therefore, the detector layout should be optimized with respect to the physics one wants to focus on. The possibility to reconfigure the detector layout to tailor to different detection needs is a specific feature of the underwater detectors. The effective area for the detection of very energetic muon neutrino fluxes ($E_\nu = 100$ TeV) can be enhanced by increasing the distance between structures. In fig. 6 the effective areas as a function of the muon energy are reported for two 9×9 detector configurations, with the same number of structures and OMs but different inter-tower distances of 140 and 300 m. A significant gain is observed for the sparser array at the expenses of a higher energy detection

threshold.

6. The NEMO Phase-1 project

In order to test technical solutions for the km^3 construction, installation and maintainance, a Phase-1 project has been realized [36]. The apparatus has been installed at the Underwater Test Site of the Laboratori Nazionali del Sud 28 km offshore Catania (Italy) at a depth pof 2000 m. An electro-optical submarine cable connects the underwater station to a shore station located inside the port of Catania. The cable system is composed by a 23 km main electro-optical cable, split at the end in two branches, each one 5 km long (Fig. 7). One branch is used for the NEMO Phase-1 experiment, while the other one provides connection for the SN-1 underwater seismic monitoring station, realized by the Istituto Nazionale di Geofisica e Vulcanologia (INGV) [41]. The NEMO Phase-1 apparatus includes all the main elements of the proposed km^3 underwater neutrino telescope: a junction box, a tower, the power transmission and a data acquisition system. The NEMO test site provides also the infrastructure for other projects operating in deep sea environment such as oceanographic research and biological survey.

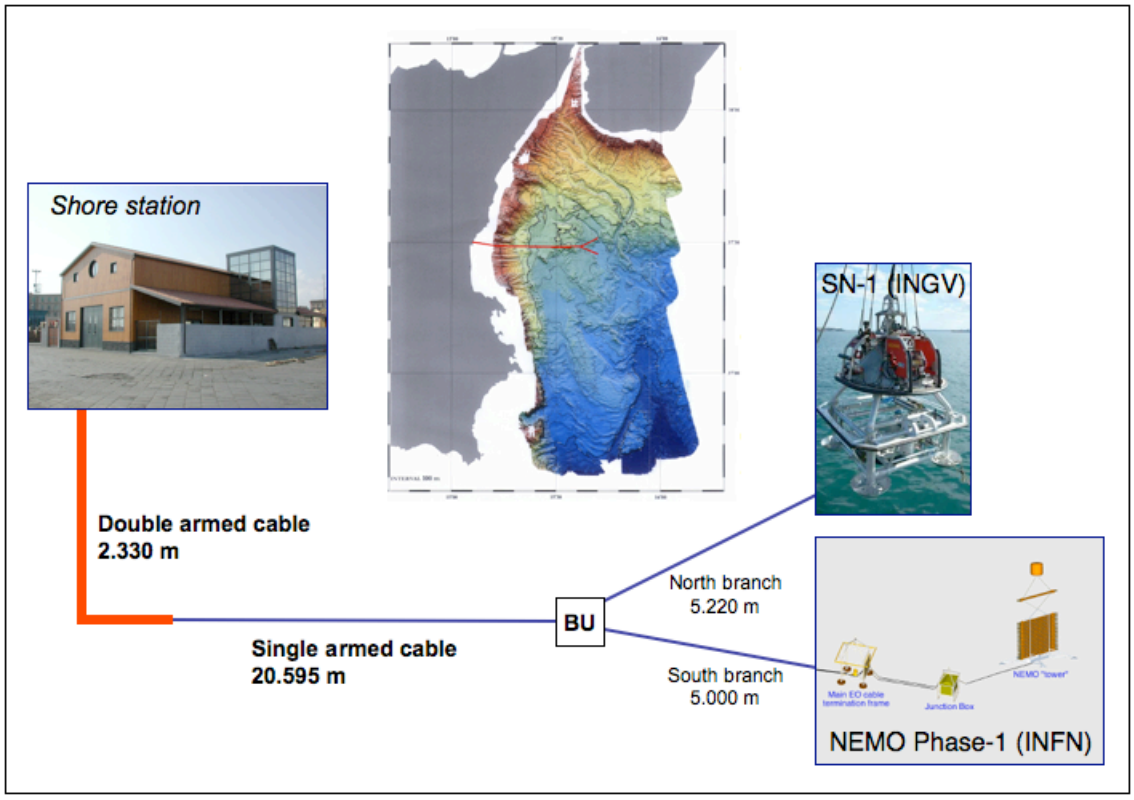

Figure 7: Scheme of the Test Site intallation and bathymetry of the area.

The Junction Box (JB) is a key element of the system and provides connection between the main electro-optical cable and the detector structures. An alternative solution with respect to the standard Titanium pressure vessels used for junction boxes operating in seawater for a long lifetime was developed. In our design the problems of pressure and corrosion resistance were decoupled.

The JB is made of four cylindrical steel vessels hosted in a large fibreglass container to avoid direct contact between steel and sea water (Figs. 8,9). The fibreglass container is filled with silicone oil and pressure compensated. All the electronics able to withstand high pressure is installed in oil bath, while the rest is located inside one pressure resistant container.

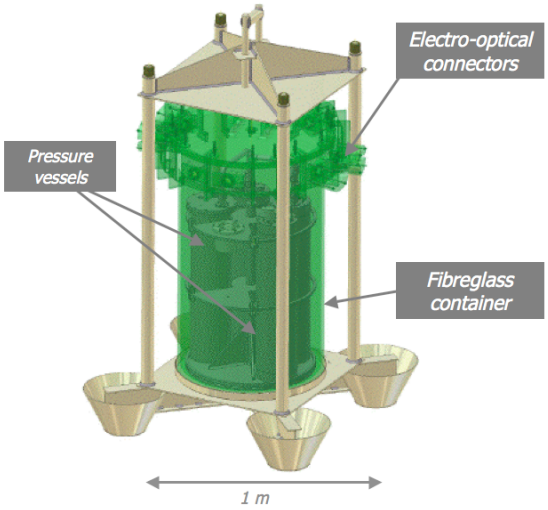

Figure 8: The NEMO Phase-1 Junction Box.

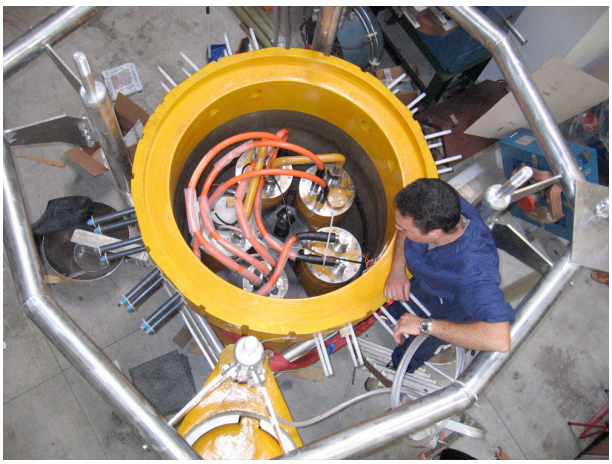

Figure 9: Top view of the Junction Box during the integration showing the support frame, the external fibreglass container and the internal vessel.

The tower that hosts the optical modules and the instrumentation is a three dimensional flexible structure composed by a sequence of floors (that host the instrumentation) interlinked by cables and anchored on the seabed. The structure is kept vertical by appropriate buoyancy on the top. While the design of a complete tower for the km^3 foresees 16 floors, a "mini-tower" of 4 floors was realized for the Phase-1 project. Each floor is made with a 15 m long structure hosting two optical modules (one down-looking and one horizontally-looking) at each end (4 OM per storey). The floors are vertically spaced by 40 m. Each floor is connected to the following one by means of

four ropes that are fastened in a way that forces each floor to take an orientation perpendicular with respect to the adjacent (top and bottom) ones. An additional spacing of 100 m is added at the base of the tower, between the tower base and the lowermost floor to allow for a sufficient water volume below the detector. In addition to the 16 Optical Modules the instrumentation installed includes several sensors for calibration and environmental deep sea monitoring. A system based on the measurements of time delays of acoustic pulses allows for the position determination of each tower element with a 10 cm accuracy. Figure 10 shows the tower on board the ship before the deployment.

Figure 10: The tower on board the ship Teliri before deployment.

The NEMO Phase-1 apparatus was installed and connected in December 2006. Figure 11 shows the deployment of the Junction Box. The apparatus has been powerd up and is presently in data taking.

7. Conclusions and outlook

The forthcoming km^3 neutrino telescopes are *discovery* detectors that could widen the knowledge of the Universe. These detectors have high potential to solve questions as the detection of UHECR sources, the investigation of hadronic processes in astrophysical environments or massive dark matter. Strong scientific motivations suggest the construction of two km^3 scale detectors in the Northern and the Southern Hemisphere. In the South Pole, following the successful experience of AMANDA, the construction of the km^3 size IceCube detector started and the completion is planned by the 2010. The realization of an underwater km^3 telescope for high energy astrophysical neutrinos represents a big challenge.

The NEMO collaboration contributed in this direction by performing an intense R&D activity. An extensive study on a 3500 m deep site close to the coast of Sicily demonstrated that it has optimal characteristics for the telescope installation. A demonstrator of the technological solutions proposed was realized. The successful installation of this prototype at the underwater Test Site of the LNS in Catania, which took place in December 2006, represents an important milestone towards the Cherenkov km^3-scale neutrino telescope in the Mediterranean Sea. Moreover, a Phase-

Figure 11: Deployment of the Junction Box.

2 project, which aims at the realization of a new infrastructure on the deep sea site of Capo Passero, started.

A further R&D program will be developed within the KM3NeT Design Study [42] in which all the European institutes currently involved in the Mediterranean neutrino astronomy projects are participating. The project, partly supported by the European Union, started in February 2006 and aims at producing a Technical Design Report for the realization of an underwater Cherenkov km^3-scale neutrino telescope in three years.

References

[1] E. Fermi, *Phys. Rev.* 75 (1949) 1169.

[2] A.R. Bell, *Monthly Not. R. Astr. Soc.* 182 (1978)147; for a description see also M.S. Longair *High Energy Astrophysics* vol.s 1 and 2, Cambridge University Press, 1994.

[3] E. Waxmann and J. Bahcall, *Phys. Rev. Lett.* 78 (1997) 2292.

[4] P.L. Biermann and P.A. Strittmatter, *Astrophys. J.* 322 (1997) 643.

[5] G.T. Zatzepin and V.A. Kuzmin, *Soviet Physics JETP Lett.* 4 (1966) 78; K. Greisen *Phys. Rev. Lett.* 16 (1966) 748.

[6] L. Costamante and G. Ghisellini *Astronomy and Astrophysics*, 56 (2002) 384.

[7] F. Aharonian et al., *Astronomy and Astrophysics* 425 (2004) L13.

[8] F. Aharonian and A.Neronov *Astrophys. J.* 619 (2005) 306.

[9] Y. Ashie et al., *Phys. Rev. Lett.* 93 (2004)101801.

[10] T.K. Gaisser, F. Halzen and T. Stanev *Phys. Rep.*, D258 (1995)173.

[11] A. Levinson and E. Waxman. *Phys. Rev. Lett.* 87 (2001) 171101.

[12] K. Mannheim, *Science* 279 (1998) 684.

[13] A. Atoyan and C. Dermer, *Phys. Rev. Lett.* 87 (2001) 221102; A. Atoyan and C. Dermer, *New Astron. Rev.* 48 (2004) 381.

[14] E. Waxman and J. Bahcall, *Astrophys. J.* 541 (2000) 707.

[15] E. Waxman and J. Bahcall, *Phys. Rev.* D59 (1999) 023001.

[16] E. Waxman and J. Bahcall, *Phys. Rev.* D64 (1999) 023002.

[17] K. Mannheim, R.J. Protheroe and J.P Rachen, *Phys. Rev.* D63 (2001) 023003.

[18] E. Waxman and K. Mannheim, *Europhysics News* 32 (2001) 6.

[19] C. Distefano et al., *Astrophys. J.* B78 (2001) 2292.

[20] P. Battacharije et G. Sigl, *Phys. Rep.* 327 (2000) 109.

[21] M.A. Markov and I.M. Zheleznykh, *Nucl. Phys.* 27 (1961) 385.

[22] R. Gandhi et al., *Phys. Rev.* D58 (1998) 93009.

[23] S. Razzaque, P. Meszaros and E. Waxman, *Phys. Rev.* D69 (2004) 023001.

[24] W. Bednarek, *Astronomy and Astrophysics* D407 (2003) 1.

[25] R. Coniglione, *Nucl. Instr. and Meth.* A 567 (2006) 489.

[26] C.D. Mobley. *Light and Water: radiative transfer in natural waters*, Academic Press, 1994.

[27] G. Riccobene for the NEMO Collaboration, *Overview over Mediterranean Optical Properties*, Proc. of the First *VLVνT Workshop*, Amsterdam, 2003, pag. 114; available at `http://www.vlvnt.nl/proceedings`

[28] E. Andres et al., *Astroparticle Phys.* 13 (2000) 1.

[29] I.A. Belolaptikov et al., *Astroparticle Phys.* 7 (1997) 263.

[30] A. Roberts et al., *Rev. of Mod. Phys.*, 64 (1992) 259.

[31] V. Aynutdinov et al., *Nucl. Instr. and Meth.* A 567 (2006) 423.

[32] J. Ahrens et al., *Astroparticle Phys.*, 20 (2004) 507; IceCube web page `http://icecube.wisc.edu`.

[33] G. Aggouras et al., *Nucl. Instr. and Meth.* A 567 (2006) 452.

[34] *ANTARES: A Deep Sea Telescoper for High Energy Neutrinos*, available at ANTARES web page `http://antares.in2p3.fr`

[35] J. Carr, *Nucl. Instr. and Meth.* A 567 (2006) 428.

[36] E. Migneco et al., *Nucl. Instr. and Meth.* A 567 (2006) 444.

[37] V. Balkanov et al., *Nucl. Instr. and Meth.* A 498 (2003) 231.

[38] D.J.L Bailey, *PhD Thesis*, University of Oxford, UK, 2003.

[39] P. Sapienza for the NEMO Collaboration, *Proceedings of the First VLVνT Workshop*, Amsterdam, 2003, pag. 114; proceedings available at `http://www.vlvnt.nl/proceedings`

[40] C. Distefano, *Nucl. Instr. and Meth.* A 567 (2006) 495.

[41] P. Favali et al., *Nucl. Instr. and Meth.* A 567 (2006) 462.

[42] U. Katz, *Nucl. Instr. and Meth.* A 567 (2006) 538.